JOURNAL
OF THE BULGARIAN GEOGRAPHICAL SOCIETY

Influence of atmospheric conditions and solar activity on the underground karst system of the Ponor Mountain

Tsvetan Parov

Space Research and Technology Institute – Bulgarian Academy of Sciences, Stara Zagora, Bulgaria
* Corresponding author: tsetsoparoov@gmail.com

Key words:
Bulgaria, cave microclimate, cave protection, geothermal energy exchange, hydrological regime, Kolkina dupka cave, surface atmosphere, underground weather

ABSTRACT

This study focuses on the meteorological parameters of the near atmosphere, the surface of the Earth and karst areas, such as temperature of water and air, relative humidity, and wind speed. These parameters are significantly influenced by solar activity, which in turn affects the temperature distribution in karst underground cavities, specifically in the "Kolkina Dupka" cave located within the Ponor Mountain of the Western Balkan Mountains range in Bulgaria. This is the deepest and longest cave in Bulgaria with a length of more than 20 km and a calculated depth of 800 m. Meteorological data within the cave was collected using data loggers, while surface weather data was sourced from National Institute of Meteorology and Hydrology of Bulgaria. Solar activity information was obtained from the website of the Royal Observatory of Belgium. The impact of solar activity on karst regions is substantial and affects temperature, precipitation, and atmospheric circulation. Changes in solar radiation can alter heat absorption on the surface of the Earth, leading to shifts in temperature and precipitation patterns. We performed statistical analysis and modeling to understand the complex interactions between Earth's near atmosphere, the karst system of the Kolkina Dupka cave, and the role of air and water flows in regulating cave temperatures. Results showed a significant negative correlation between air temperatures in the deep underground airflows (at a depth of 130 m below the surface) and temperatures at the cave entrance (at a depth of 40 m during the winter months. Conversely, during spring and summer, an intriguing reversal occurs where higher external temperatures are linked to increased air temperatures at the cave entrance, accompanied by lower temperatures in the deeper zone. Furthermore, by employing "lagged correlations" in result analysis, investigating correlations between internal temperatures and external temperatures over the preceding and subsequent seven days, cyclic variations in heat exchange between the near-surface atmospheric layer and the underground temperatures within the karst system were observed. Specifically, a consistent temperature elevation was noted at the cave entrance three days prior to an increase in external temperatures during the spring-summer season. This temporal relationship was also observed in the solar activity data, where an increase in temperature at a depth of -40 m was registered three days prior to the escalation of solar activity within the measured range of 2800 MHz. The obtained results formed the basis for the development of new theories in solar-terrestrial physics. In summary, there is a connection between solar activity and Earth's climate, but it is not a direct and simple correlation, and it is just one piece of the larger puzzle that shapes temperature variations of the Earth. Climate science involves studying these interactions over extended periods to gain a more comprehensive understanding of the climate system of the Earth.

Article processing
Submitted: 15 October 2023
Accepted: 25 November 2023
Published: 08 December 2023
Academic editor: Stoyan Nedkov

1. Introduction

Solar-terrestrial physics examines the way in which the Sun influences Earth on various time scales. Long-term changes in Earth's atmosphere resulting from variations in solar activity and climate changes are observed in ocean sediments (Ho and McClymont 2023), polar glaciers (Steinhilber et al. 2012), and cave formations (Wong and Breecker 2015). A better understanding of changes in speleoclimate and the distribution of heat fluxes in karst mountains is of great importance for various engineering aspects: tunneling, mining, geothermal studies, cave development, water management (Temelkova 2018) and ecosystem services assessments (Stefanov et al 2023). The exploration of the underground world has only been developing for about 100 years. In Bulgaria, the relationship between cave temperatures (Uhlovitsa, Snezhanka, Sueva Dupka, and Ledenika caves) and changes in solar activity has been studied for 40 years (Stoeva and Stoev 2005). In addition to climate parameter studies, monitoring of radon gas and carbon dioxide in the Chelevechnitsa Cave in the Rhodope Mountains has been added (Kyurkchiev 2019). Previous research is made in horizontal and relatively easily accessible caves and provides the foundation for the beginning of the study of the vertical and multi-level cave system of Kolkina Dupka, which is the deepest and longest cave in Bulgaria, and a much of it remains unexplored and unmapped.

This research aims to investigate and present the response of deep vertical underground air volumes and water flows relative to external climatic changes and variations in solar activity. This knowledge can serve as the foundation for the construction of the first human bases in the other planets in Solar System.

2. Material and methods

2.1 Case study area

Ponor Mountain is located in the central part of the Western Stara Planina mountain range. This mountain is an impressive karst region characterized by a flat relief and a catchment area of 140 km² (Dinev 1959). The areas with elevations ranging from 1100 to 1300 m above sea level have the widest spatial distribution, featuring extensive and relatively flat meadows. Ponor Mountain is situated between the Petrohan Pass and the Ginska River to the west, the Iskar River to the east, and is bounded by the Kozlya and Iskretska Rivers to the south, and the Koznishki Rid and Proboinitsa River to the north. The mountain is sparsely populated, with settlements mainly located on its periphery. For years, this mountain has attracted many researchers, but it is of particular interest to hydrogeologists and speleologists. Easy access and closeness to Sofia provide opportunities for its thorough exploration and study.

In geological terms, it can be said that the mountain is composed of rocks formed during the Lower Paleozoic and Mesozoic eras. Ponor Mountain is formed by limestone and dolomites and represents one of the biggest and most characteristic karst areas in Bulgaria. The water penetrating the calcareous rocks has created large negative Karst forms like whirlpools, potholes (ponor in Bulgarian), and blind valleys. More than 70 caves have been found in the Ponor massif but the longest and deepest are Katsite cave (depth 205 m, length 2560 m and altitude of entrance 1245 m) and Kolkina dupka (depth 542 m, length 19164 m, altitude of entrance 1285 m). Both caves provide drainage of underground waters of more than 10 km (along a straight line) to the springs near the village of Gara Bov (Fig. 1).

In hydrogeological terms, the area of Ponor Mountain is very interesting. Several surface rivers flow in the northern parts of the mountain, whose waters are entirely lost in sinkholes and nourish the springs on the periphery of the karst massif. The largest springs are the Iskrets Springs, with their discharge varying within wide limits, ranging from 260 to 35,900 l/s (Paskalev et al. 1992). Other smaller springs are located in villages Tserovo and Gara Bov, with much smaller but also variable discharges. The waters from all these springs are the subject of numerous hydrogeological studies (Dinev 1959; Benderev 1989), as they are used for water supply purposes.

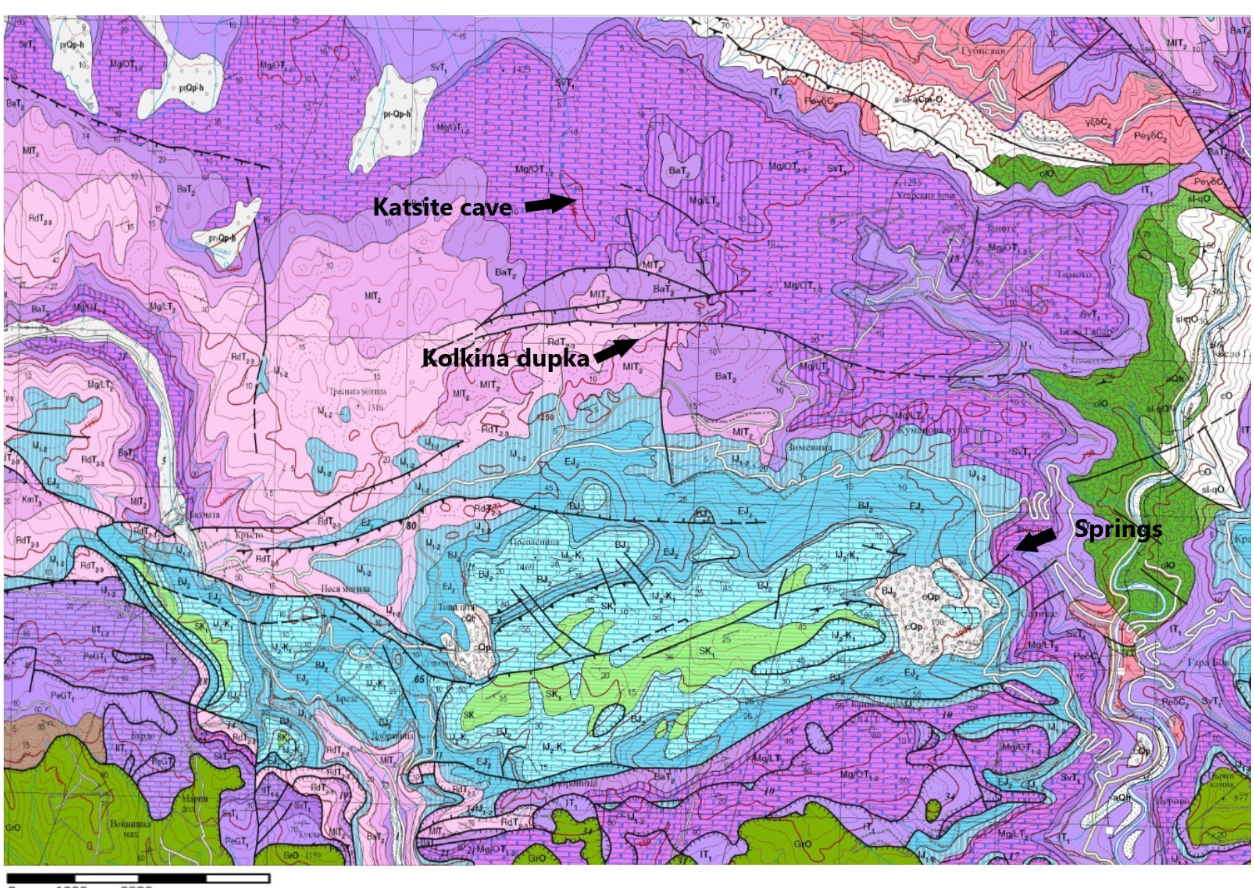

Figure 1. Geological profile of Ponor Mountain according to the Geological Map of Bulgaria, scale 1:50000, M 1:50 000, K-34-35-G (Lakatnik) (Angelov et al. 2008)

Of particular interest to our research were the springs above Bov train station, where it had been proven through dye tracing with fluorescein that the waters emerging at the surface originate from the "Kolkina Dupka" cave.

The total elevation difference that overcomes the underground river is about 800-850 m., with the length of the galleries traversed by humans exceeding 20 km (Official site of caving club Pod Rb—Tserovo village 2023). This provides a basis for the creation of thermodynamic circulation of large air masses between the Iskar River Valley and the slopes of Ponor Mountain. The dissolution of soluble rocks creates a network of underground channels and voids through which water flows. Solar radiation can increase the temperature of surface water flows, leading to increased evaporation and water loss. This can have implications for water availability and quality in karst areas. Solar radiation is a key driver of energy transfer in the Earth's system. It provides the energy necessary for photosynthesis, evaporation, and precipitation. The amount and intensity of solar radiation that reaches the Earth's surface are influenced by factors such as latitude, season, and atmospheric conditions.

The statement that the temperature in caves is constant (Badino 2005a) (Caves are often described as having a constant temperature. The reason is that rock is slow to transmit heat.). applies to dry, small and/or closed cave systems that have reached a blocked-cementation stage of their development, where the absence of incoming water streams and blocked airflow leads to the rock and its geothermal flux being the primary sources of heat.

2.2. Time and Location

This research started on 28.12.2022 as a long-term monitoring with the placement of two data loggers with built-in sensors Comet U4130 for recording of temperature, humidity, and atmospheric pressure. The sensors were configured to record readings every 60 min. The positioning of the sensors was determined through participation in five expeditions conducted in the cave during the year 2022. Finally, two points were selected. The first point is located 40 m vertically from the entrance of the cave (S40), where the noticeable boundary between the external surface atmosphere and the underground atmosphere is present. Also, the point was selected in such a way that it is far away from an underground river. The second measurement point (S130) was chosen at approximately 100 m vertically and around 120 m horizontally from the first point, within the presumed zone of constant temperatures. The sensor was placed at the uppermost point of an inclined underground chamber with dimensions: length of 50 m, width of 20 m and a height of approximately 10 m. At the lowest point of the chamber, an underground river appears. To prevent condensation formation we placed the devices in protective enclosures. At the end of July 2023, two additional sensors (Tinytag Aquatic 2) were installed to measure the water temperature of the underground river. The first one was placed where the underground river is initially encountered at the point -180 m. vertically from the surface, and the second one was installed at the springs where the underground river emerges to the surface. The data from the water temperature measurement sensors will be downloaded at the beginning of 2024. The sensor data was manually downloaded using a cable and a computer. For this purpose, two additional expeditions were conducted in the cave in March 2023, April, and July 2023. Unfortunately, during the winter season, the protection against sensor condensation proved to be insufficient, and the high humidity led to the rapid depletion of their batteries. The sensor at a depth of -130 (S130) meters operated for 38 days, while the sensor at a depth of -40 (S40) meters collected data for 60 days. The sensors were removed and serviced, and more suitable anti-condensation enclosures were installed before they were returned to the cave. The locations for placing the underground sensors are marked on Fig. 2.

2.3. Solar activity

Indicator of solar activity is the radio emission flux from the Sun at a wavelength of 10.7 cm (frequency of 2.8 GHz). The 2.8 GHz or 10.7 cm solar radio flux has long been monitored as a representative indicator of solar radio activity since 1946, currently by Dominion Radio Astrophysical Observatory in Penticton, Canada (Tapping and Charrois 1994). It is an important indicator of solar activity because it tends to track changes in the solar ultraviolet range, which impacts the upper layers of Earth's atmosphere and ionosphere. Many models of Earth's upper atmosphere use the 10.7 cm flux (F10.7) as input to determine atmospheric density and satellite resistance. F10.7 has been shown to closely follow the number of solar spots and similar techniques can be used for forecasting. The information about the solar activity we take from the monthly bulletin of Royal observatory of Belgium (Royal Observatory of Belgium 2023).

2.4. Surface meteo parameters

The daily values for external temperature, precipitation amount, and wind speed in the area of Ponor Mountain were provided by the National Institute of Meteorology and Hydrology-Sofia city. The amount of precipitation was measured once a day and covered a period of 24 hours. It was measured in liters per square meter or millimeters.

2.5. Surface reflection and absorption of heat, moisture, and forest condition

For surface visualization of the dry and deforested area of the Ponor Mountain, we utilized the Sentinel-2 platform (Fig. 3). The False color images are a representation of a multi-spectral image produced using bands other than visible red, green and blue as the red, green and blue components of an image display. False color composites allow us to visualize wavelengths that the human eye can not see (i.e. near-infrared). It is most commonly used to assess plant density and health, as plants reflect near infrared and green light, while absorbing red. Since they reflect more near infrared than green, plant-covered land appears deep red. Denser plant growth is darker red. Cities and exposed ground are gray or tan, and water appears blue or black. The study of albedo and absorbed heat will be included in the research in 2024.

3. Data analyses

To process the obtained data tables containing more than 3000 hourly collected values of various meteorological parameters, we conducted Pearson correlations (SPSS 2023) (two-tailed and cross-correlations) using the statistical software SPSS to investigate the statistical relationships between temperatures at different depths (S40 and S130) in the cave and surface meteorological parameters for both winter and summer seasons. To search for cyclic atmospheric phenomena in the datasets, we employed PYTHON programming language procedures, comparing each day's measurements with those from seven days prior and seven days ahead. LagResults are tables of delayed correlations, i.e., the correlation between internal variables and external ones from the previous day, from two days ago, and so on up to seven days. There are also reverse correlations, denoted with (-), representing the internal variables from previous days with external ones from the following days. We use them to compare the air temperature in the cave before and after precipitation.

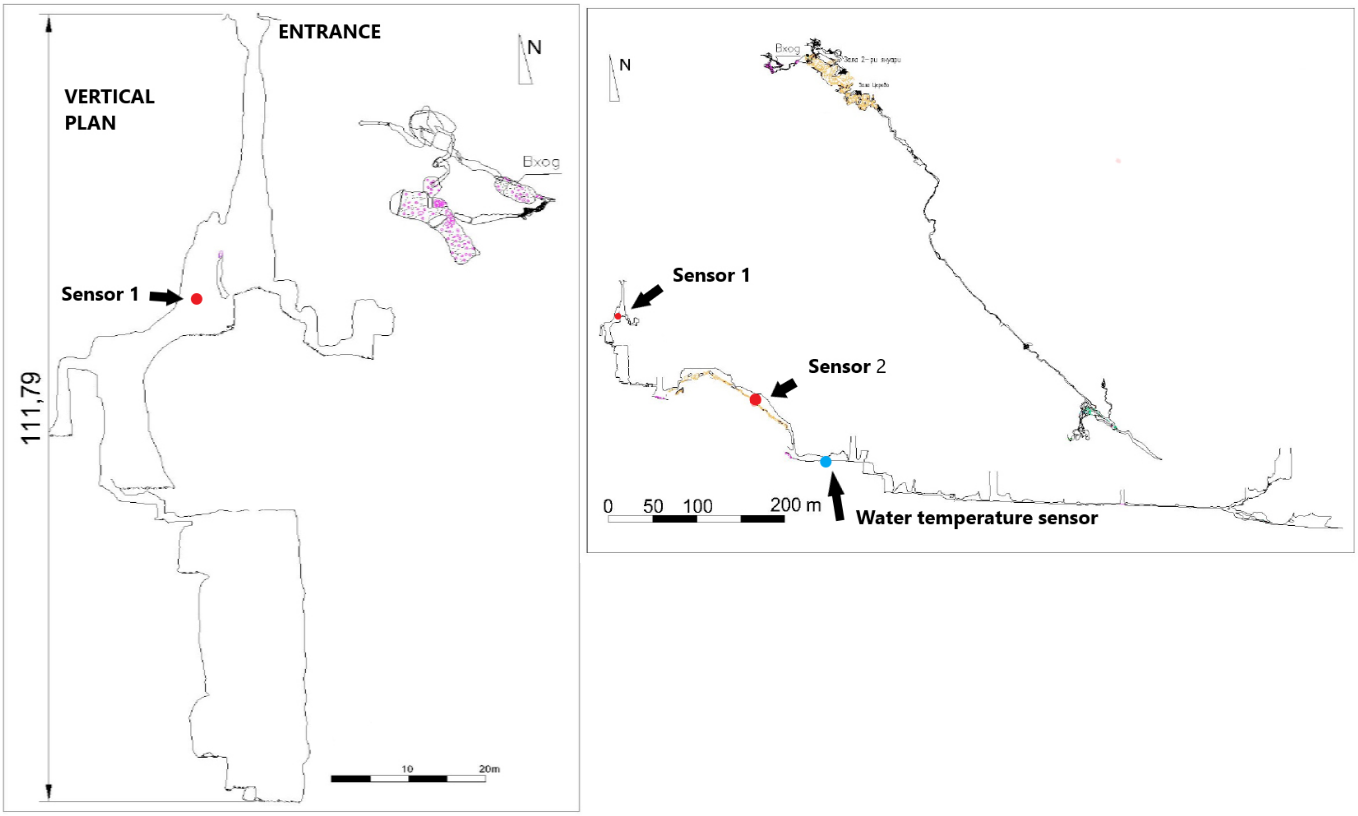

Figure 2. Red spots-sensors S40 and S130, blue spot-water temperature sensor (W180).

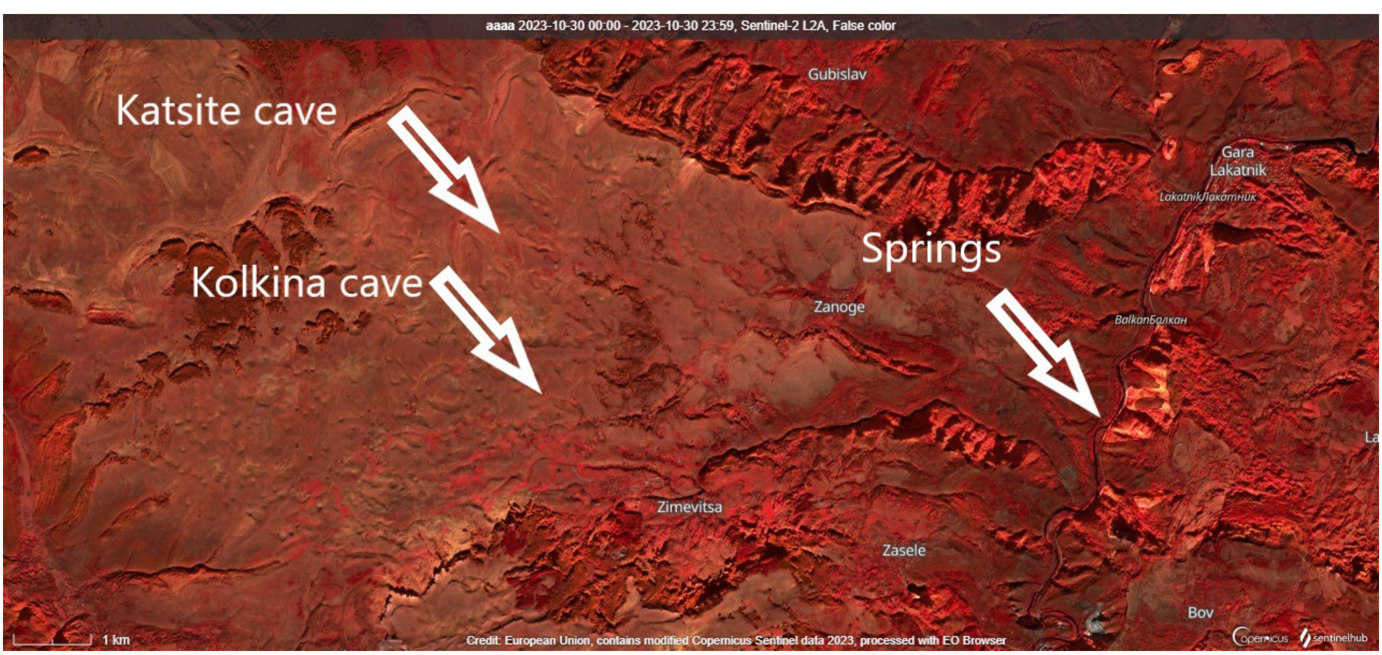

Figure 3. Sentinel-2 Satellite platform - infrared False color of Ponor mountain.

3. Results

3.1. Temperature in cave and amount of precipitation

The winter season of 2023 was characterized by positive temperatures and a lack of snow cover in January, followed by low temperatures and mainly icy surfaces in February (National Institute of Meteorology and Hydrology 2023). Overall, January in the Ponor Mountain area saw little precipitation, except for January 7th when about 20 l/m² fell in one day and January 19th when 50 l/m² fell in three days (Fig. 4) (National Institute of Meteorology and Hydrology 2023). From the temperature graphs of S130 for January, an obvious influence on the temperature in the deep parts of the cave is observed (where an underground river passes near the sensor). Regarding precipitation and its impact on cave temperature, we performed the following steps: For each day, we calculated the average temperatures at S40 and S130 for three days ahead and three days back (including the current day). Then, we selected only rainy days ("Rain" > 0) and conducted an independent two-sample t-test.

Paired-Sample t-Test Results for 'S_130_average_before' and 'S_130_average_after'
Mean Before: 10.32°C, Mean After: 10.71°C
$t = -1.42$, $p = 0.214$, Degrees of Freedom: 5

The average temperature for S130 the three days prior was 10.32°C, while for the three days following, it was 10.71°C.

For the shallow sensor, which is located far from groundwater sources and therefore exposed to lower relative humidity values, we were fortunate that it operated for 60 days (Fig. 5). Due to its distance from the underground rivers, the drier part of the cave filters out the weak temperature fluctuations caused by lighter precipitation and only registers the amount of heat introduced by heavy rainfall with a flow rate exceeding 20 l/m² In January, in the days preceding heavy rainfall, surface temperatures on Ponor Mountain reach 15°C.

Paired-Sample t-Test Results for 'S_40_average_before' and 'S_40_average_after'
Mean Before: 9.68°C, Mean After: 9.83°C
$t = -3.48$, $p = 0.007$, Degrees of Freedom: 9

The average temperature for S40 the three days before rain is 9.68°C, and for the three days following is 9.83°C.

We have high significance during the winter (January 2023–March 2023).

During the summer measurement session from April 2023 to July 2023, there were exceptionally many rainy days where, through statistical methods, we observed minimal temperature fluctuations. Changes of 0.01°C at the surface of the Earth do not have a significant impact, whereas in a humid cave climate saturated with water vapor, they can be crucial in shifting the dew point and condensation processes (Badino 2005b) During the exceptionally rainy months of May and June, we observed an increase of one hundredth of a degree in the temperature of S130 after rainfall (Fig. 6).

Paired-Sample t-Test Results for 'S_130_average_before' and 'S_130_average_after'
Mean Before: 9.56°C, Mean After: 9.57°C
$t = -1.26$, $p = 0.214$, Degrees of Freedom: 44

However, there is a clear correlation between the seasonal rise in surface temperatures (July with temperatures around 20–25°C and the increase in the temperature of S40. The proximity to the surface neutralizes the effects of heat transfer due to precipitation (Fig. 7).

Paired-Sample t-Test Results for 'S_40_average_before' and 'S_40_average_after'
Mean Before: 9.65°C, Mean After: 9.63°C
$t = 0.84$, $p = 0.405$, Degrees of Freedom: 44.

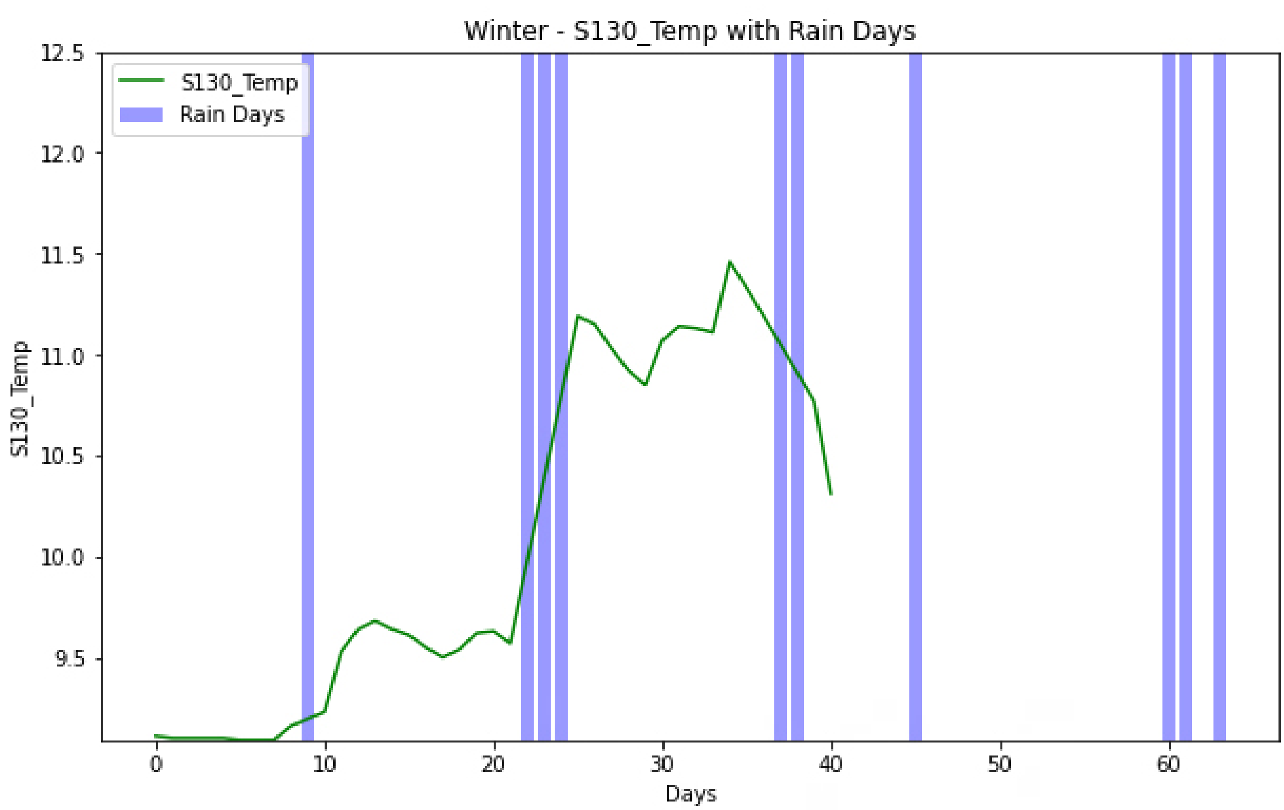

Figure 4. Temperature of Sensor 130 and rain days.

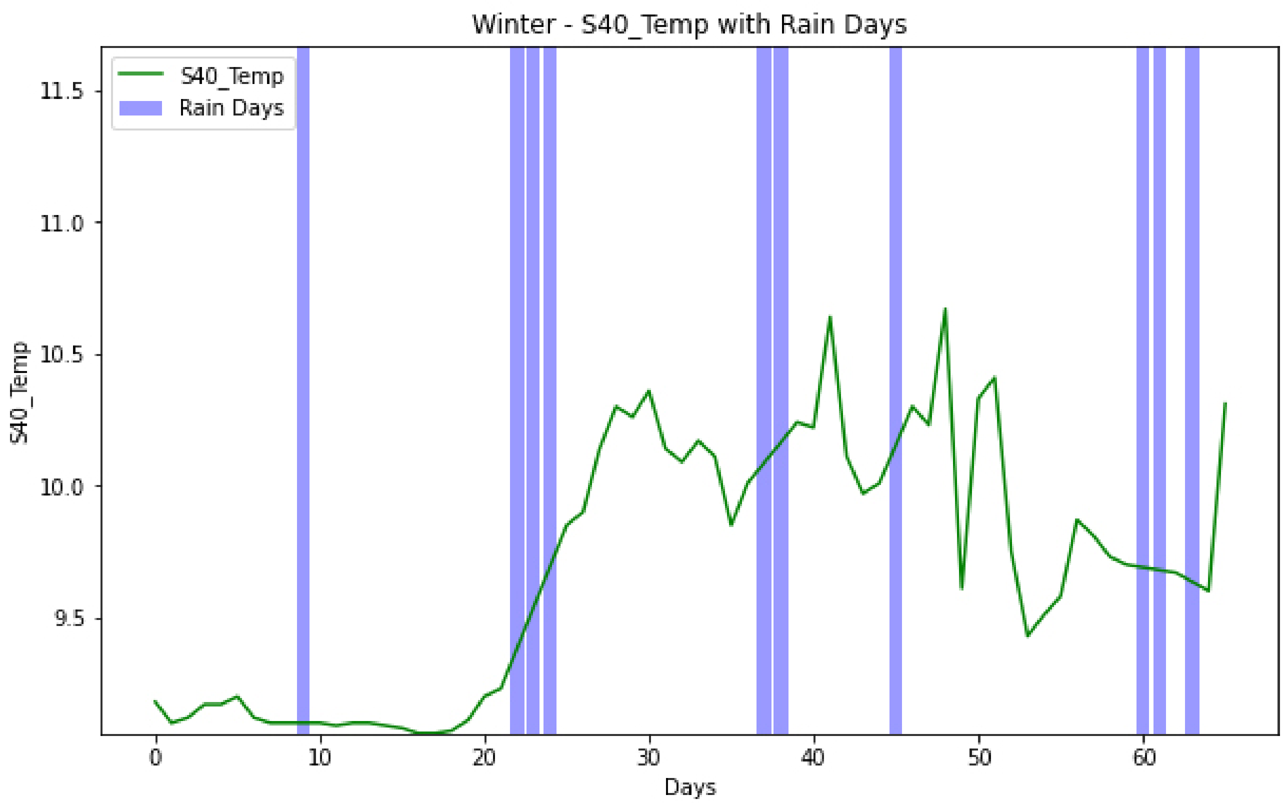

Figure 5. Temperature of Sensor 40 and rain days.

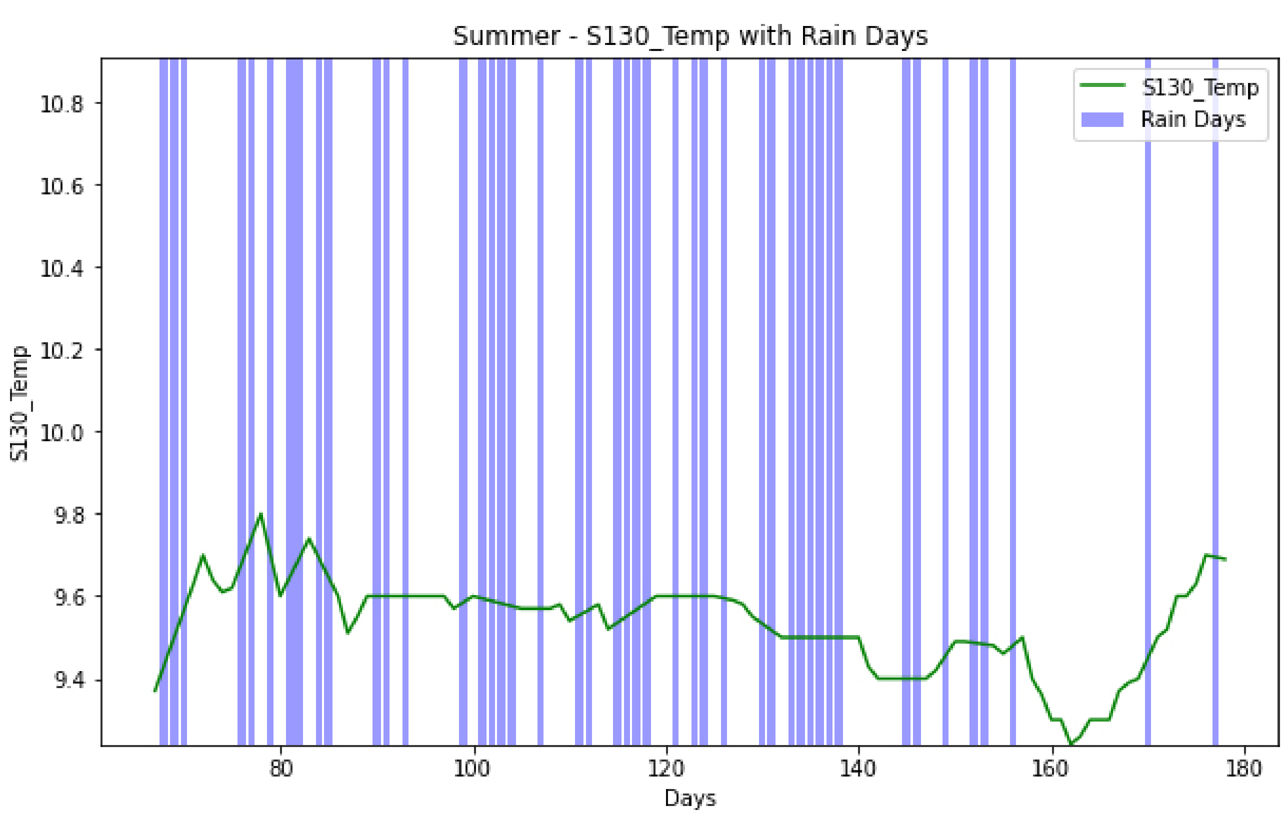

Figure 6. Temperature of Sensor 130 and rain days.

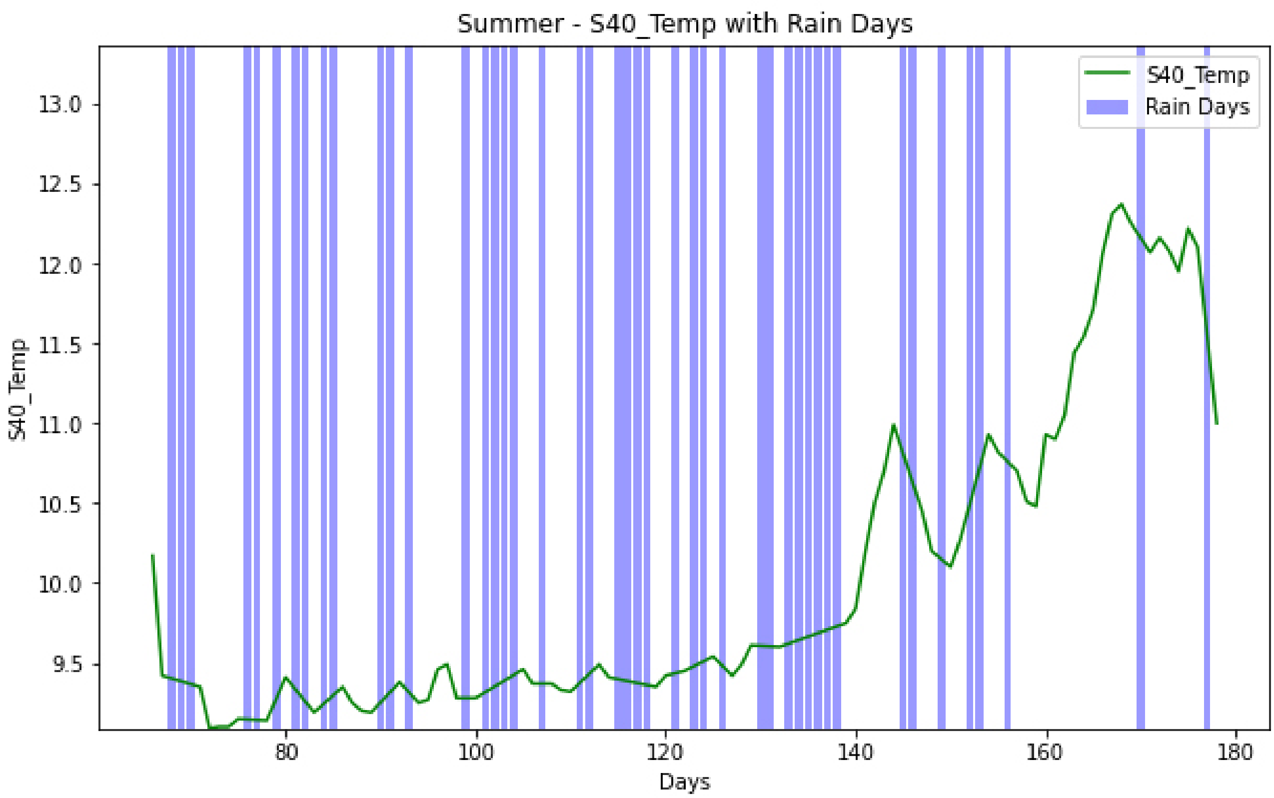

Figure 7. Temperature of Sensor 40 and rain days.

4.2 Temperature in cave (Temp S130, Temp S40) and outside temperature (Temp_)

The Pearson correlations (p) between the external temperature (Temp) and all other variables (Table 1). Here are the lag results of comparing each day of the study with seven days ago and seven days ahead, with only the most significant correlations included, where their maximum always occurs on the third day (Table 2):

Day 3: Maximum correlation observed between the variables.

Day 4: Correlation decreases compared to Day 3 but remains significant.

Day 2 and Day 5: Correlations also significant but lower than on Day 3.

Day 1, Day 6, and Day 7: Correlations continue to decrease and are the least significant in the study.

The interesting ones: The external temperature correlates positively with that of the shallow sensor and negatively with that of the deep one (Fig. 8 and Fig. 9). This holds true for 3 days ahead and 3 days back.

Table 1. Pearson correlations (p) between the external temperature (Temp) and all other variables for the summer.

Pearson correlation coefficient	Value
"p" between outside Temp and Sun Spots index:	0.564366
"P" for outside Temp and Sun Frequency of 2.8 GHz:	0.624566
"P" for outside Temp and S130_Temp:	-0.584568
"P" for outside Temp and S40_Temp:	0.800119

Table 2. Lag Results for 3 days +/-.

Pearson correlation coefficient	Value
S130_Temp_Lag3	-0.678662
S130_Temp_Lag-3	-0.559663
S40_Temp_Lag3	0.723887
S40_Temp_Lag-3	0.829797

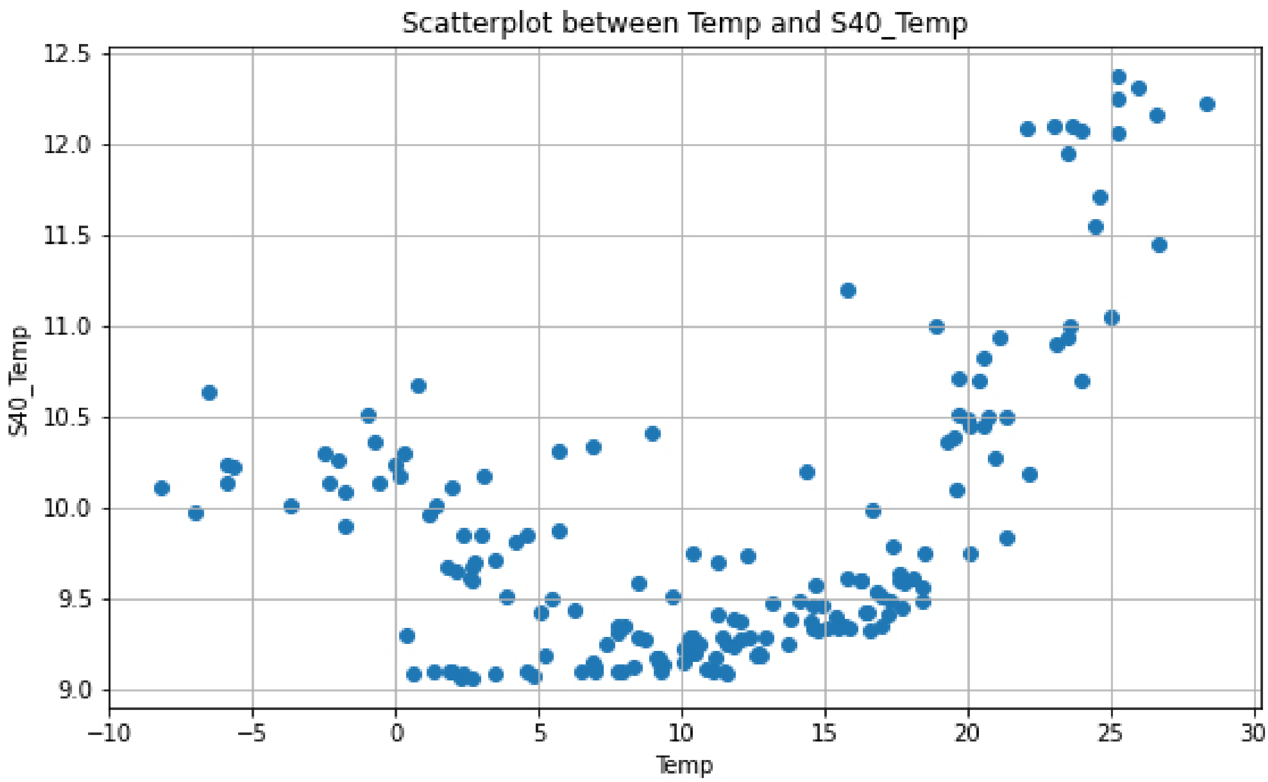

Figure 8. Graphical representation of the correlation between external temperature (Temp) and internal temperature (temp S40). One point represents one day.

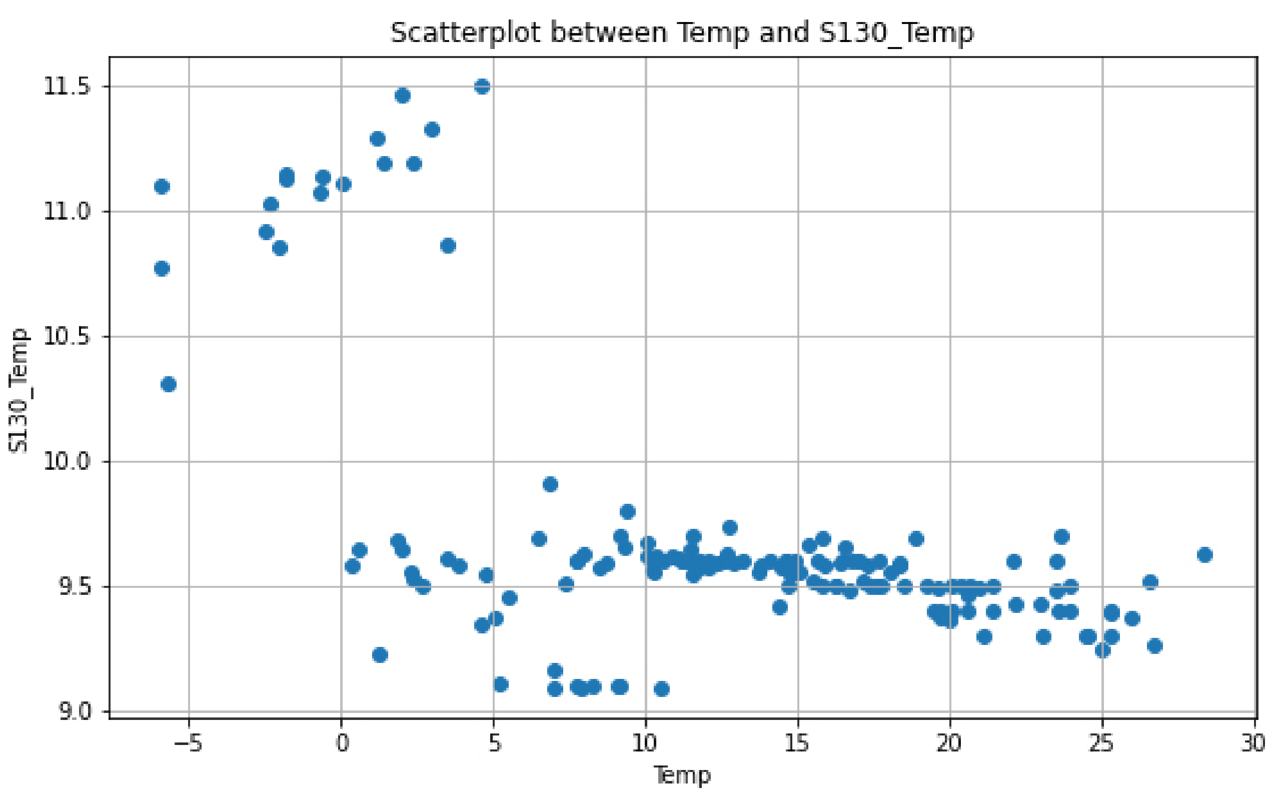

Figure 9. Graphical representation of the correlation between external temperature (Temp) and internal temperature (temp S130). One point represents one day.

The main reason for temperature fluctuation in Kolkina Dupka cave is certainly the incoming water flows, which is heavily influenced by the quantity and temperature of precipitation. The second reason is the incoming air flow, which exhibits cyclic and reversible movement patterns, which we will further investigate by installing anemometers in 2024. Water flux dominated thermal exchanges because the greater heat capacity. For pure water, the specific heat capacity is approximately 4.18 J/g°C or 1 cal/g°C. This means that it takes 4.18 joules of energy to raise the temperature of 1 gram of water by 1 degree Celsius. Water's relatively high heat capacity is why it can absorb and store a significant amount of heat energy, making it important in various natural processes and applications, such as regulating Earth's climate and in heating and cooling systems. The heat capacity of air with water vapor is a more complex parameter because it depends on the relative humidity (RH) (the amount of water vapor in the air, in Kolkina dupka cave we measured 98-100% RH) and the temperature. It is typically calculated using a mixture approach, taking into account the heat capacities of dry air and water vapor separately. The specific heat capacity of dry air at constant pressure (Cp) is approximately 1.006 kJ/kg°C. The specific heat capacity of water vapor at constant pressure is approximately 1.996 kJ/kg°C. To calculate the heat capacity of moist air (air with water vapor), you would use a weighted average based on the specific humidity (mass of water vapor per unit mass of dry air) and the heat capacities of dry air and water vapor. The formula for calculating the heat capacity of moist air is:

Cp(moist air) = Cp(dry air) + (specific humidity) * Cp(water vapor)

Where:

Cp(moist air) is the heat capacity of moist air.

Cp(dry air) is the heat capacity of dry air.

Specific humidity is the mass of water vapor per unit mass of dry air.

Cp(water vapor) is the heat capacity of water vapor.

Keep in mind that the specific humidity and temperature of the air can vary, so the heat capacity of moist air will also vary under different conditions.

For the winter:

The outside temperature during winter correlates negatively with that of both internal sensors. In other words, when surface temperatures rise, internal temperatures decrease. Where the lag file name is positive (_lag3) (Table 3), internal data is delayed. In other words, external temperature precedes internal temperature. The opposite is true for negative values (_lag-3) (Table 4).

It is true that in some cases, there is a higher correlation with the lags than without them, but it's not fundamentally different. It's also true that external temperature, especially during winter, is not so stable.

4.3 Study and interaction between temperatures in the entrance part of the cave (S40 meters) and the deep parts (S130 meters)

For winter, there is a positive Pearson correlation of p=0.89 between S40 and S130.

During the winter, when at the entrance's elevation of the cave (1300 m a.s.l. the temperature is low (during our measurements in January– February 2023, reaching as low as -15°C), inside the cave, the atmosphere is significantly warmer (~9°C) and consequently has a lower density. This causes the ascent of air currents within the mountain massif. However, these air movements are constrained by heat exchange with the external atmosphere due to the pressure of the surface cold air inversion. This results in a reduction in relative humidity, which is a function of the mixing of two saturated airflows with different temperatures.

For summer, we observed a negative correlation of p=-0.537, which means that when the sensor at -40 m temperature increases, the temperature at depth -130 decreases (Figs. 10, 11). This phenomenon can be explained by considering that the atmosphere inside the cave is denser and colder compared to the surface. As a result, the underground air masses "sink" downward, and in the process, they "draw in" warm air from the surface. This leads to a noticeable increase in humidity and the amount of condensed water on the cave walls.

Table 3. Pearson correlations (p) between the outside temperature (Temp) and all other variables for the winter.

Pearson correlation coefficient	Value
"p" between outside Temp and Sun Spots	0.111024
"p" between outside Temp and Sun Frequency	0.026695
"p" between outside Temp and S130_Temp	0.647297
"p" between outside Temp and S40_Temp	0.544902

Table 4. Lag Results for 3 days +/-.

Pearson correlation coefficient	Value
S130_Temp_Lag3	-0.714367
S130_Temp_Lag-3	-0.465519
S40_Temp_Lag3	-0.427206
S40_Temp_Lag-3	-0.554904
Temp_Lag3	0.554964
Temp_Lag-3	0.554964

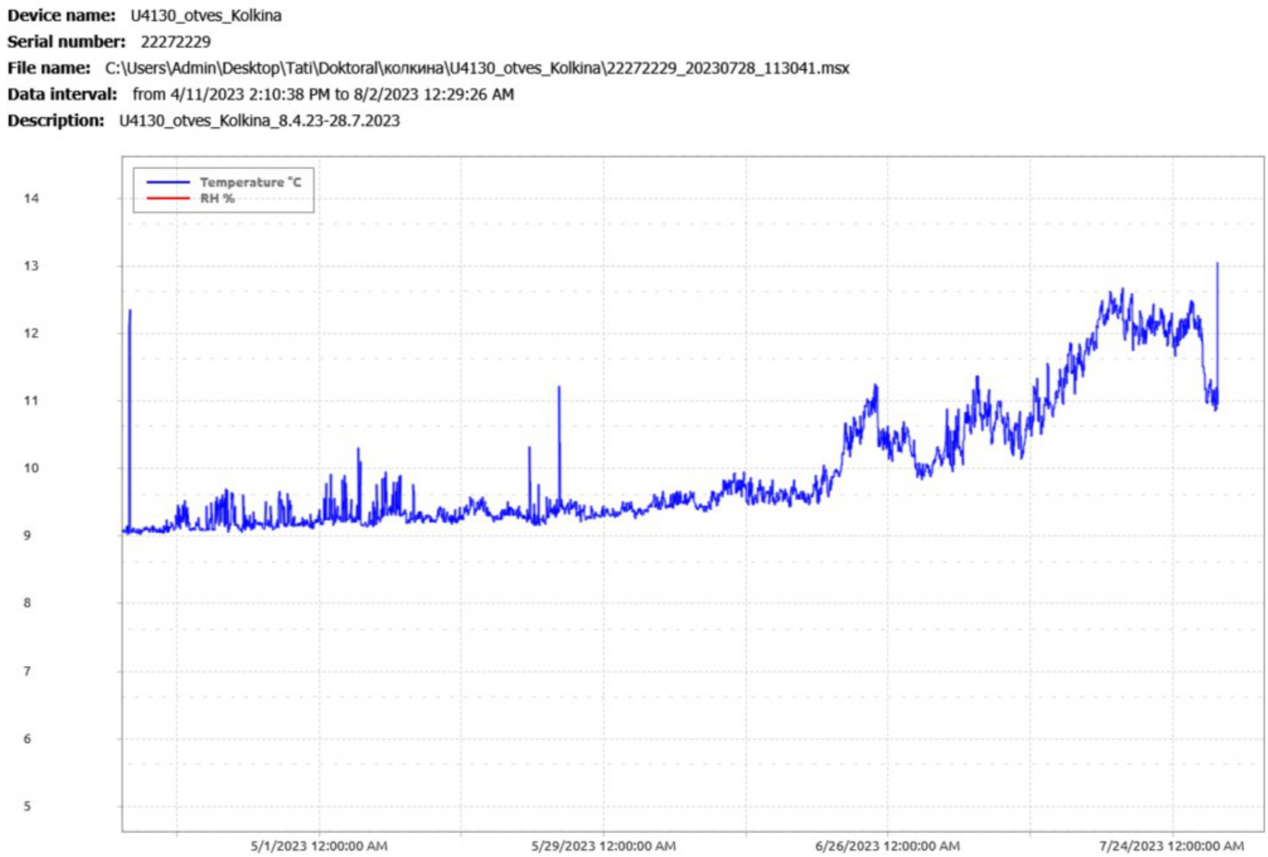

Figure 10. Temperature for the summer: April–July for S40.

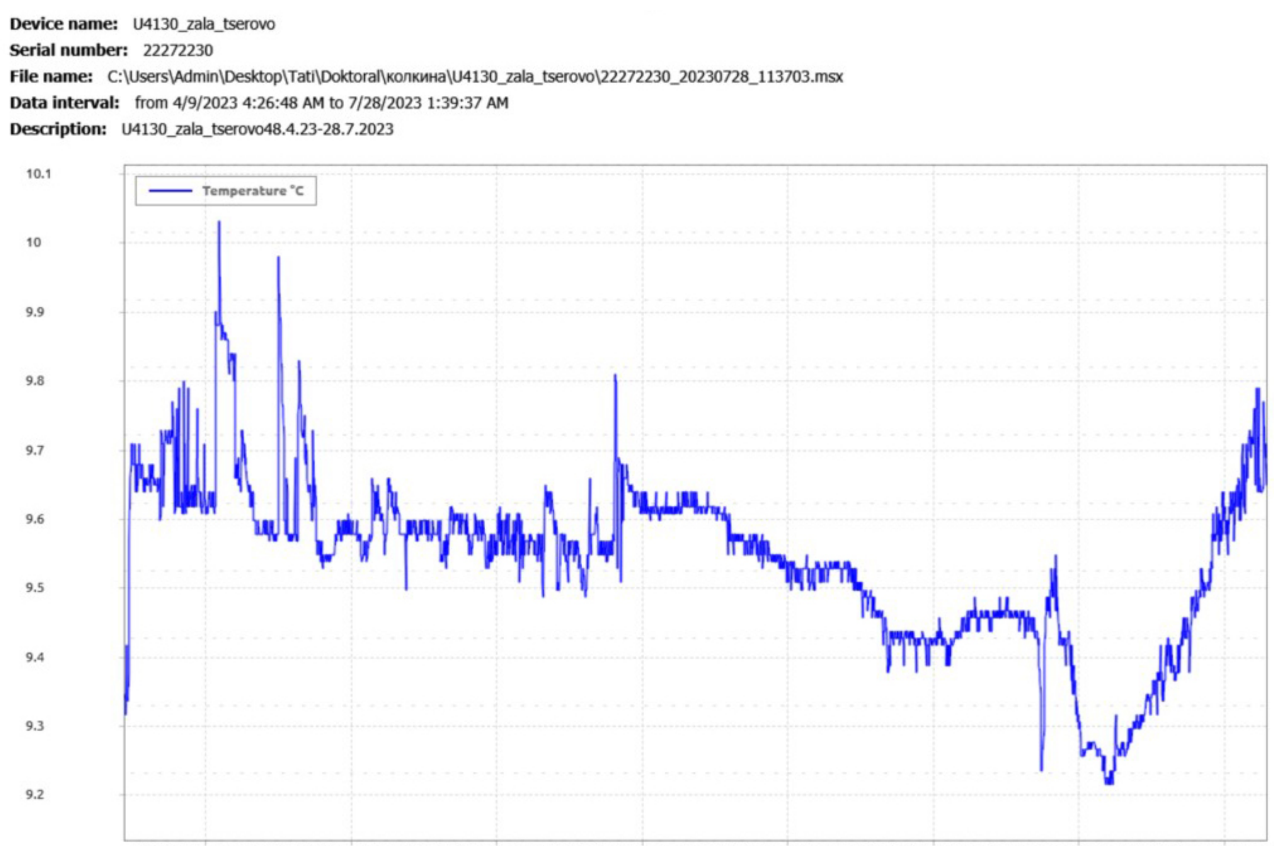

Figure 11. Temperature for the summer: April–July for S130.

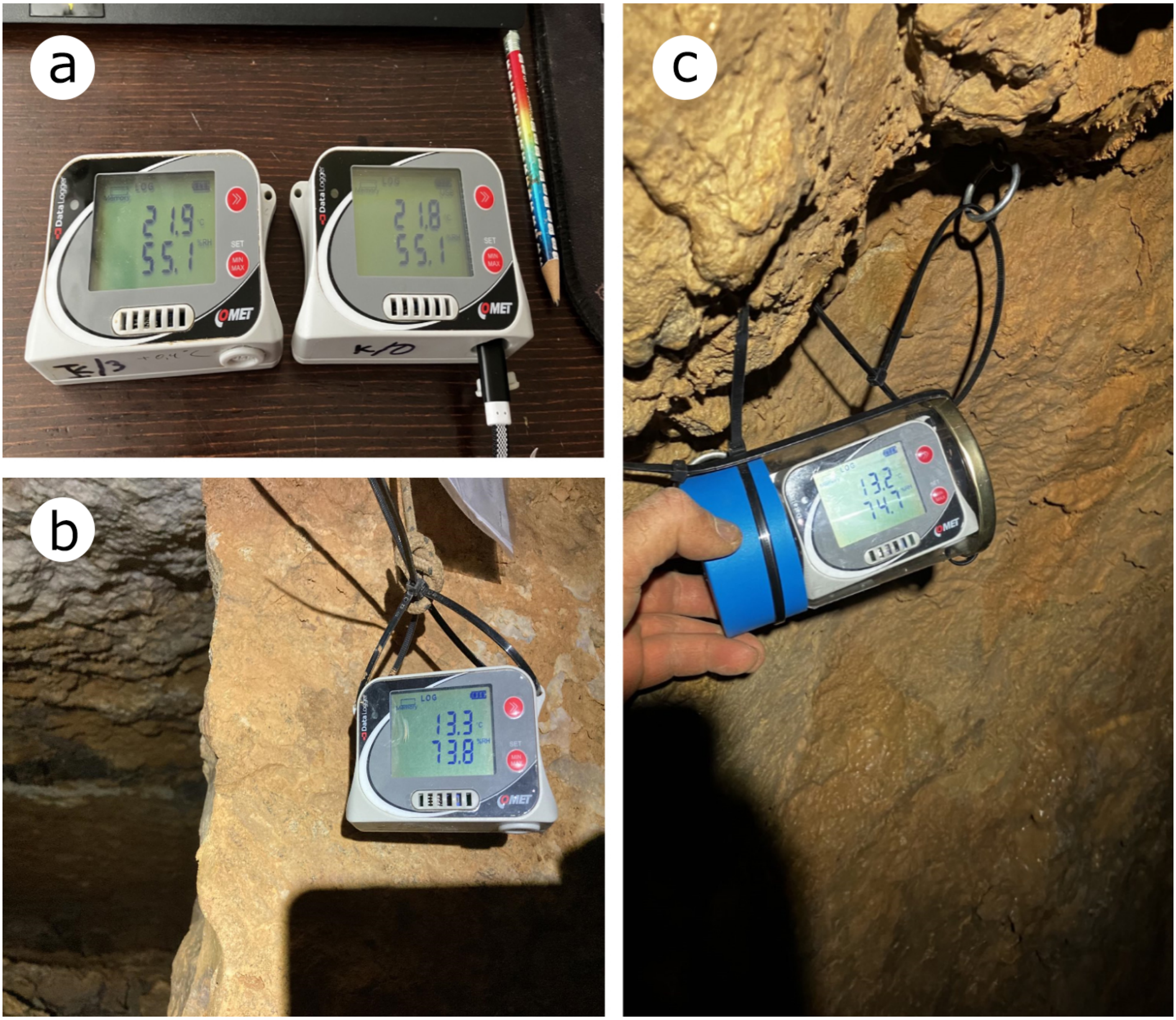

Figure 12. Data loggers for temperature, pressure, relative humidity. **A** Cross calibration to equalize values, **B** Position in cave without cover, **C** Position in cave after upgrade.

5. Discussion

Our preliminary results show that temperature fluctuations in the studied large and deep underground system are not influenced by the geothermal flux but rather depend on the relationship between the cave temperature, which is influenced by the rock temperature, which, in turn, depends on the temperature of the passing waters significantly affected by surface conditions and also change during the pathway of underground water through the cave. The temperature gradient determines a difference of about 5°C between the air temperature at the cave entrance and the springs and both with the difference in atmospheric pressure create continuous movement of air masses in underground volumes.

Unfortunately, during the winter measuring season, the sensor (S130) only operates for 38 days before its battery gets damaged (Fig. 4). To improve moisture resistance, the author created protective cases and placed the sensors inside (Fig.12)

This article presents the first results of the research into the relationships and interactions between the climatic physical parameters within the depths of the karst system developed beneath Ponor Mountain and the surface climate. In addition to this research, solar activity is also being considered, but for accurate results and analysis, we require the monitoring and recording of data over an entire solar cycle, which spans 11 years. Fortunately, at the outset of data collection, the current solar cycle (Solar cycle 25) is in its ascending phase, with expectations of reaching the maximum of solar spots in 2025.

This phenomenon for three days forward and backward may simply be related to the stability of all temperatures over a long period of time. This is why direct correlations between external temperature and its own lags are shown—some stability is evident.

An interesting fact, during the summer is that three days before an increase in solar activity in the 2800 MHz radio index, the cave's input sections register a rise in temperature. Perhaps it should simply be noted as an intriguing observation without making definitive conclusions until further investigation and examination of additional parameters are conducted!

We will have a more comprehensive understanding of the thermodynamic fluctuations of underground and surface streams in 2024 when we have information on the temperature gradient of the underground rivers. This information will be obtained thanks to the two underwater temperature data loggers placed in the cave in July 2023. Additionally, we expect to install an ultrasonic anemometer in March 2024 to determine the speed and volume of the air currents. The data from the water temperature measurement sensors will be downloaded at the beginning of 2024 and this will be added to the study.

In simpler terms, the behavior of the two main fluids in a cave, water and air, is fundamentally different. Water mainly flows downward and at the lowest points of the cave passages. Because water can store a lot of heat, it has a significant influence on underground temperatures. However, its movement doesn't preserve heat, and it tends to absorb energy from the underground environment. On the other hand, air can move freely in all directions within the cave, even changing its flow direction. This flexibility allows air to have a substantial impact on temperature exchanges. Air can also make the cave walls damp, and its moisture content helps stabilize temperature fluctuations and has a dominant role in energy transfers. Importantly, as air moves through the cave, it undergoes continuous temperature changes, and there is ongoing heat exchange between the air and water.

Acknowledgements

This study would not have started without the support and voluntary efforts of the cavers from the “Pod Rb”–Tserovo cave club, especially the caver Pavlin Dimitrov for the professional and safety underground support. Special thanks also go to the geologists Svetoslav Marinov and Yordanka Donkova for the geological advice and guidance.

References

Angelov V, Antonov M, Gerdjikov S, Aydanliiski G, Petrov P, Kiselinov H (2008) Geological Map of Bulgaria in scale M 1:50 000, K-34-35-G (Lakatnik) map sheet. Apis 50, Sofia.

Badino G (2005a) Underground Drainage Systems and Geothermal Flux. Acta Carsologica 34(2): 277–316. https://doi.org/10.3986/ac.v34i2.261

Badino G (2005b) Clouds in Caves. Speleogenesis and Evolution of Karst Aquifers. Speleogenesis and evolution of karst aquifers 2(2). https://speleogenesis.com/pdf/seka_pdf4499.pdf

Benderev A (1989) Karst and karst waters in Ponor mountain. PhD Thesis. Geology Committee, Sofia, Bulgaria

Wong CI, Breecker DO (2015) Advancements in the use of speleothems as climate archives. Quaternary Science Reviews 127: 1-18. https://doi.org/10.1016/j.quascirev.2015.07.019

Dinev P (1959) An attempt to determine the hydrogeological catchment of the Iskrets Karst Springs. In: Karst Groundwaters in Bulgaria. Tehnika, Sofia, 162–182.

Steinhilber F, Abreu JA, Beer J, Brunner I, Christl M, Fischer H, Heikkilä U, Kubik PW, Mann M, McCracken KG, Miller H, Miyahara H, Oerter H, Wilhelms F (2012) 9,400 years of cosmic radiation and solar activity from ice cores and tree rings. Proceedings of the National Academy of Sciences 109(16): 5967-5971. https://doi.org/10.1073/pnas.1118965109

Ho SL, McClymont E (2023) Marine Sediments Reveal Past Climate Responses to CO2 Changes. https://doi.org/10.1029/2023EO235027

Kyurkchiev S (2019) Microclimatic characteristic of the Chelevechnitsata cave in Western Rhodopes. Journal of the Bulgarian Geographical Society 41: 10-17. https://doi.org/10.3897/jbgs.2019.41.2

Paskalev M, Benderev A, Shanov S (1992) Tectonic conditions of the region of the Iskrets karst springs (West Stara Planina). Review of the Bulgarian Geological Society 53(2): 69–81. https://bgd.bg/REVIEW_BGS/REVIEW_BGD_1992_2/PDF/07_Paskalev.pdf

Stoeva P, Stoev A (2005) Cave air temperature response to climate and solar and geomagnetic activity. Memorie della Societa Astronomica Italiana 76: 1042–1047. http://sait.oat.ts.astro.it/MmSAI/76/PDF/1042.pdf

Stefanov P, Prodanova H, Stefanova D, Stoycheva V, Petkova G (2023) Monitoring of water cycle in karst geosystems and its integration into ecosystem assessment framework. Journal of the Bulgarian Geographical Society 48: 15-26. https://doi.org/10.3897/jbgs.e101301

Tapping KF, Charrois DP (1994) Limits to the accuracy of the 10.7 cm flux. Solar Physics 150: 305–315. https://doi.org/10.1007/BF00712892

Temelkova M (2018) Karst Waters in Northwestern Bulgaria. Journal of the Bulgarian Geographical Society 39: 35-40. https://doi.org/10.3897/jbgs.2018.39.6

Official site of caving club Pod Rb—Tserovo village https://pod-rb.eu/ (2023)

Royal Observatory of Belgium, Sunspots Bulletin. https://www.sidc.be/SILSO/sunspotbulletin (2023)

SPSS, Pearson correlation. https://libguides.library.kent.edu/spss/pearsoncorr (2023)

National Institute of Meteorology and Hydrology http://www.weather.bg/ (2023)

Conflict of interest

The author has declared that no competing interests exist.

ORCID

https://orcid.org/0009-0005-2865-1600 - T. Parov